

Inelastic electron tunneling spectroscopy of a single nuclear spin

F. Delgado and J. Fernández-Rossier

Departamento de Física Aplicada, Universidad de Alicante, San Vicente del Raspeig, 03690 Spain

(Dated: February 16, 2022)

Detection of a single nuclear spin constitutes an outstanding problem in different fields of physics such as quantum computing or magnetic imaging. Here we show that the energy levels of a single nuclear spin can be measured by means of inelastic electron tunneling spectroscopy (IETS). We consider two different systems, a magnetic adatom probed with STM and a single Bi dopant in a Silicon nanotransistor. We find that the hyperfine coupling opens new transport channels which can be resolved at experimentally accessible temperatures. Our simulations evince that IETS yield information about the occupation of the nuclear spin states, paving the way towards transport-detected single nuclear spin resonance.

PACS numbers:

Probing a single nuclear spin represents both the ultimate resolution limit of magnetic resonance imaging and a requirement in quantum computing proposals where the nuclear spin is used as a qubit. The idea of storing and manipulating information in nuclear spins goes back to quantum computing proposals based on P donors in Si[1] and NMR quantum computing [2]. Because of their very small coupling to their environment, the nuclear spin coherence time is expected to be very long but, for the same reason, quantum measurement of a single nuclear spin remains a formidable task. Recent experimental breakthroughs have made it possible to perform single shot non-destructive measurement of a single nuclear spin by means of optically detected single spin magnetic resonance in NV centers in diamond [3].

Here we propose a setup based on inelastic electron tunneling spectroscopy (IETS) that would permit to probe the spin transitions of a single nuclear spin with a space resolution down to 1 Å outperforming in this particular regard the optical detection. Our proposal builds on recent progress to probe the spin of a single atom using two different strategies. On one side, Scanning Tunneling Microscope (STM) inelastic electron tunnel spectroscopy [4–10] which allow to measure the electron spin spectral function of a single magnetic atom [11] weakly coupled to a conducting substrate. On the other side, the fabrication of a Silicon nanotransistor where transport occurs through the electronic states of a single dopant[12, 13].

In STM-IETS experiment electrons tunnel between the tip and the conducting substrate going through the magnetic atom. As the bias voltage V is increased, a new conduction channel opens whenever eV is larger than the energy of some internal excitation of the atom. In the case of isolated transition metal atoms with partially full d shell, like Mn, Fe or Co, the only internal excitations available in the range of a few meV are spin excitations associated to the magnetocrystalline anisotropy [6, 11]. In the case of the single dopant nanotransistor, the IETS of the electron spin in the donor level could be performed in the cotunneling regime[14].

Exchange coupling to nearby magnetic atoms affects significantly the spin excitation spectrum of the atom under the tip [5, 8, 9, 11]. Hyperfine coupling to the nuclear spin should also result in a modification of the electronic spin spectral function which, in turn, could be probed in IETS provided that the spectral resolution is high enough. Our mechanism differs from earlier theory work [15, 16] proposing to detect the nuclear spin looking at its influence on the STM current noise spectrum. Their approach is based on previous experiments where electronic spin fluctuations are detected in the current noise spectra[17], not in the conductivity spectra. Probing the spin transitions of a single nuclear spin would yield a completely unambiguous chemical identification of the atom and would be a first step towards transport-based quantum measurement of a single nuclear spin.

The rest of this letter is organized as follows. We first describe the general theory that relates nuclear spin flips to IETS transport features. Then we consider the archetypical case of a single Mn atom in a Cu₂N surface [4–6, 9]. We find that the detection of the nuclear spin excitations could be done at 4mK, below the recently demonstrated 10mK experimental limit [18], and how the visibility can be enhanced driving the nuclear spin out of equilibrium. We then analyze the case of ²⁰⁹Bi in Silicon and we find it is an optimal system to observe single nuclear spin flips at temperatures up to 60mK.

The electronic spin S and nuclear total angular momentum I are described by a Hamiltonian $\mathcal{H}_0(S, I)$ whose eigenvalues and eigenvectors are denoted by ϵ_M and $|M\rangle = \sum_{I_z, S_z} \Psi_M(I_z, S_z) |I_z\rangle |S_z\rangle$, where $|I_z\rangle |S_z\rangle$ is the basis in which both electronic and nuclear spin have well defined projection along the z axis. The spin mixing coefficients $\Psi_M(I_z, S_z)$ depend on the specifics of the Hamiltonian, described below, which includes hyperfine coupling, Zeeman coupling and magnetic anisotropy terms. The inelastic transport spectroscopy is sensitive to transitions between states M and M' with excitation energy $\Delta_{M',M} = \epsilon_{M'} - \epsilon_M$. The electronic spin is coupled to electrons in the electrodes, denoted as tip (source) and

the surface (drain) in the STM (nanotransistor) geometry, through a Kondo-like Hamiltonian[11, 19–21]:

$$\mathcal{V} = \sum_{\alpha, \lambda, \lambda', \sigma, \sigma'} T_{\lambda, \lambda', \alpha} \frac{\tau_{\sigma\sigma'}^{(\alpha)}}{2} \hat{S}_\alpha c_{\lambda, \sigma}^\dagger c_{\lambda', \sigma'}, \quad (1)$$

where both electrode conserving and electrode non-conserving exchange couplings are included. The operator $c_{\lambda, \sigma}^\dagger$ creates an electron with spin σ and orbital quantum number $\lambda = \eta, \vec{k}$, where $\eta = T, S$ labels the electrode and \vec{k} the wave vector. The index α runs over $a = x, y, z$, with $\tau^{(a)}$ and \hat{S}_a the Pauli matrices and the atom electronic spin operators respectively. The $\alpha = 0$ term (with $\tau^{(0)}$ and \hat{S}_0 the identity matrix) corresponds to potential scattering. We assume that exchange is momentum independent, spin isotropic and electrode dependent: $T_{\lambda, \lambda', a} \equiv v_\eta v_{\eta'} \mathcal{T}$. Here v_η are dimensionless parameters that account for the different coupling between the magnetic adatom and either the tip or the surface[21, 22].

The inelastic current due to electronic-spin assisted tunneling I_{in} can be expressed[11] as a convolution of the electronic spin spectral function:

$$\mathcal{S}(\omega) \equiv \sum_{M, M', a} P_M \left| \hat{S}_a^{M, M'} \right|^2 \delta(\hbar\omega - \Delta_{M', M}) \quad (2)$$

where P_M denotes the average occupation of the state M and $\hat{S}_a^{M, M'} = \langle M | \hat{S}_a | M' \rangle$. The inelastic current can be written as [11, 22]:

$$I_{\text{in}}(V) = \frac{g_0}{G_0} \sum_{M, M', a} P_M(V) \left| \hat{S}_a^{M, M'} \right|^2 i(\Delta_{M, M'} + eV). \quad (3)$$

Here $g_0 \equiv \frac{\pi^2}{4} G_0 \rho_T \rho_S |\mathcal{T} v_T v_S|^2$ is the tunneling conductance, $G_0 = 2e^2/h$ is the quantum of conductance and ρ_η the density of states of the η electrode at the Fermi level. The inelastic current associated to a single channel is given by $(e/G_0)i(\Delta + eV) = \mathcal{G}(\Delta + eV) - \mathcal{G}(\Delta - eV)$, with $\mathcal{G}(\omega) \equiv \omega (1 - e^{-\beta\omega})^{-1}$ and $\beta = 1/k_B T$.

Importantly, $\frac{d\mathcal{G}(\Delta + eV)}{dV}$ has a step at $eV = \Delta$ that accounts for the characteristic dI/dV lineshape. Thus, whenever the bias energy eV exceeds a transition energy between spin states with $\Delta_{M', M} = eV$ such that the initial state is occupied, $P_M > 0$, and the electronic spin flip transition is permitted, $\hat{S}_a^{M, M'} \neq 0$, the differential conductance dI/dV has a step and d^2I/dV^2 has a peak (or a valley at negative bias) with a thermal broadening[23] of $\Gamma_{k_B T} \equiv 5.4 k_B T$. Thus, the d^2I/V^2 line-shape should be quite similar to the electronic spin spectral function $\mathcal{S}(eV)$. In the following we assume that the intrinsic broadening of the spin excitations, due for instance to their coupling to the conducting substrate[21, 22, 24], is negligible compared to $\Gamma_{k_B T}$, as it happens in the case of Mn adatoms in Cu_2N [9, 22, 24].

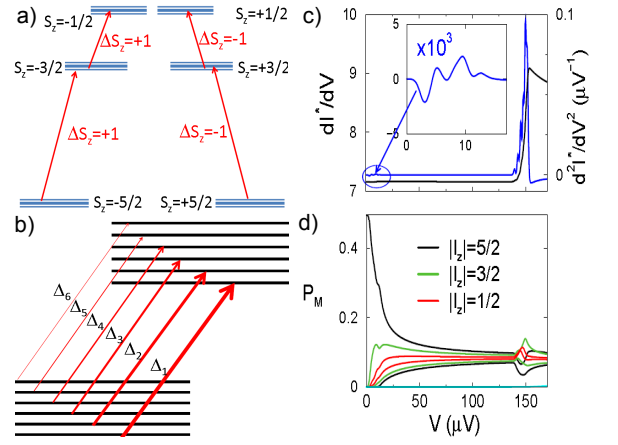


FIG. 1: (a) Energy level scheme of the $^{55}\text{Mn}^{2+}$ adatom on the Cu_2N surface. (b) Detail of the $S_z = 5/2 \rightarrow 3/2$ transition with resolved hyperfine structure. (c) dI^*/dV and d^2I^*/dV^2 in the high current regime ($v_T = v_S = 1$) at $T = 4\text{mK}$ ($I^* = I/g_0$). Inset: magnified low bias d^2I^*/dV^2 . (d) Corresponding occupations of each of the 12 lowest energy electronic nuclear eigenstates of $\mathcal{H}_0(S, I)$ for the $^{55}\text{Mn}^{2+}$ versus applied bias.

The occupation functions P_M can differ substantially from those of equilibrium when the typical time elapsed between inelastic current events is shorter than the spin relaxation time [21, 22]. We determine the occupation functions P_M by solving a master equation[21, 22] that accounts for the dissipative dynamics of the current driven electronic spin interacting with the nuclear spin. Both energy and spin are exchanged between the electrons in the electrodes on one side, and the nuclear and electronic spin of the single atom on the other. The scattering events involve the creation or annihilation of an electron-hole either in the same electrode, in which case no current is involved, or in different electrodes. Thus, P_M depends in general, on the voltage, the conductance and the temperature [22].

We now address the main question of this letter: under which conditions would IETS reveal transitions that provide information about the nuclear spin state?. We first consider the case of a single Mn adatom in a Cu_2N surface. This system has been widely studied experimentally and theoretically[5, 6, 9, 11, 20–22, 24, 25] but the role of the nuclear spin has been overlooked so far. The single atom electronic spin can be described by means of a spin $S = 5/2$ Hamiltonian,

$$\mathcal{H}_S = DS_z^2 + E(S_x^2 - S_y^2) + g_e \mu_B \vec{B} \cdot \vec{S} \quad (4)$$

where $D = -39\mu\text{eV}$ and $E = 7\mu\text{eV}$ account for the uniaxial and in-plane anisotropy respectively, whereas the third term describes the electronic Zeeman coupling. At zero magnetic field the experimental[6] dI/dV features a step at an energy of $\Delta \simeq 4|D|$ associated to electronic

spin flip between the two ground states which neglecting E , have $S_z = \pm 5/2$ and the first excited states, with $S_z = \pm 3/2$, see Fig. 1(a). The only stable nuclear isotope of Mn is ^{55}Mn and has a nuclear spin of $I = 5/2$, so that the electronic-nuclear system has 36 states in total. The hyperfine structure associated to the coupling between I and S has been resolved with EPR and NMR experiments that address ensembles of more than 10^{12} atoms, and can be described by a Heisenberg-type coupling. So, the spin Hamiltonian reads as

$$\mathcal{H}_0(S, I) = \mathcal{H}_S + A \vec{S} \cdot \vec{I} \quad (5)$$

The strength of the hyperfine coupling A depends both on the nuclear magnetic moment and on the shape of the electronic cloud, which is environment dependent. In the case of Mn, A varies between 0.3 and $1\mu\text{eV}$ [26]. Here we take $A = 1\mu\text{eV}$. The effect of the hyperfine coupling is to split each of the 6 electronic levels into 6 nuclear branches, as observed in Fig. 1a,b). The lowest electronic multiplet, corresponds to the $S_z = \pm 5/2$, while the $S_z = \pm 3/2$ and $S_z = \pm 1/2$ branches are found approximately at $4|D|$ and $6|D|$ above.

The discussion can be simplified if we take advantage of the fact that $|D| \gg E, A$ so that the eigenstates of $\mathcal{H}_0(S, I)$ have, to zeroth order in E and A , well defined projection of the electronic (S_z) and nuclear (I_z) spin, although the numerical calculations are done with the exact states. The energies are approximately given by $E_0(S_z, I_z) = DS_z^2 + AS_z I_z + g\mu_B S_z$. We find two kind of transitions: low energy excitations with $\Delta S_z \simeq 0$ and higher energy excitations with $\Delta I_z \simeq 0, \Delta S_z = \pm 1$. The former are found at small bias $eV \simeq S_z A \Delta I_z$, where ΔI_z is the change in nuclear spin. Whereas these transitions yield very weak peaks in $d^2 I/dV^2$, shown in Fig. 1d), they contribute to drive the nuclear spin out of equilibrium, as seen in Fig. 3a).

In contrast, the electronic spin transitions between the electronic ground states $\pm 5/2$ and the first excited states $\pm 3/2$ that, to zeroth order, conserve the nuclear spin, occur at higher $eV \simeq 4|D|$ and have a much stronger signal (Fig. 1c,d) and 2). At $B = 0$ their energies are given by $\Delta_{\pm}(I_z) = 4|D| \pm A I_z$ so that, the hyperfine coupling splits the lowest energy line of the electronic spin spectral function into 6 lines separated by $A = \Delta_{\pm}(I_z) - \Delta_{\pm}(I_z \pm 1)$. In order to have a thermal broadening smaller than A , $k_B T$ must be reduced down to $\simeq 0.2\mu\text{eV}$ ($T \simeq 2\text{mK}$), which would deplete the thermal occupation of the higher energy nuclear states within the electronic ground state, and the visibility of the corresponding spin excitations. In contrast, by decreasing the tip-atom distance [9] it is possible to drive the system out of equilibrium and populate also the higher energy nuclear spin states at low temperatures, as shown in Fig. 1d), which makes it possible to observe all the transitions, as seen in Fig. 2 even at $T = 4\text{mK}$.

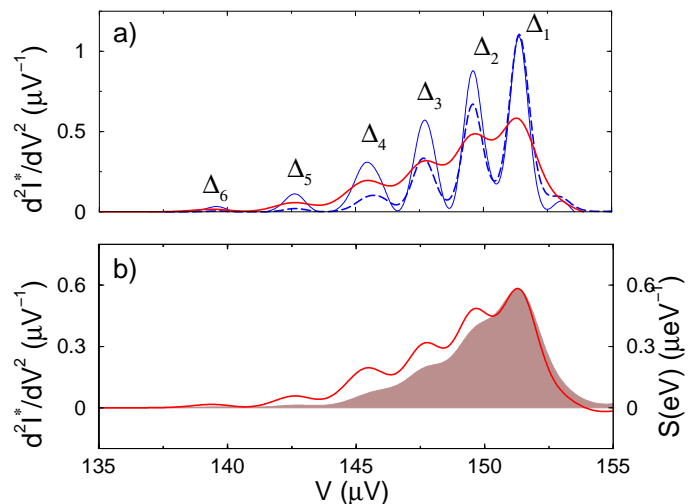


FIG. 2: (Color online) Conduction spectrum $d^2 I^*/dV^2$ as a function of applied bias ($I^* = I/g_0$). (a) Spectra for $T = 4\text{mK}$ (thick solid line) and $T = 2\text{mK}$ (thin solid line) with $v_T = v_S = 1$ (far from thermal equilibrium) and $T = 2\text{mK}$ (thick-dashed line) with $10v_T = v_S = 1$ (close to thermal equilibrium). (b) $d^2 I/dV^2$ for $T = 4\text{mK}$ and $v_T = v_S = 1$ (solid line) and spin spectral function $S(\text{eV})$ as a function of applied bias (dashed line).

In figure 2b) we plot $d^2 I/dV^2$ together with the electronic spin spectral function $S(\text{eV})$, where the occupations P_M evaluated at eV and the delta function replaced by $\frac{d^2 i}{dV}$. It is apparent that $d^2 I/dV^2$ and $S(\text{eV})$ are related. Importantly, the spin spectral function contains information not only about the energy levels of the joint nuclear-electronic spin, but also about the occupations of the states. Thus, the height of the $d^2 I/dV^2$ can be correlated with the occupations of the nuclear spin states, outperforming current-noise spectroscopy[15, 16]. This indicates that it would be possible to use IETS-STM as a detector in a magnetic resonance experiment, in analogy with the optically detected single spin magnetic resonance. This would permit to probe the magnetic field with subatomic spatial resolution and accuracy afforded by the linewidth of nuclear resonance experiment.

Nuclear spins with larger hyperfine coupling, like Yb, Er or Pr, [27, 28] could be probed with IETS at higher temperatures than Mn. For instance $^{167}\text{Er}^{3+}$ in Y_2SiO_5 [27] can have A up to $6\mu\text{eV}$. The case of ^{232}Bi in Silicon is particularly interesting. This system attracts a lot of interest[29, 30] in the context of quantum computing based on the nuclear spin of donors[1] where addressing the nuclear spin of a single dopant is required. The hyperfine coupling between the $I = 9/2$ nuclear spin and the electronic spin of the donor state is quite large, $A = 6.1\mu\text{eV}$ (1.48GHz)[29, 30]. The zero field Hamiltonian $A\vec{I} \cdot \vec{S}$ can be diagonalized in terms of the total angular operator F , resulting in two multiplets ($F=4, F=5$) with en-

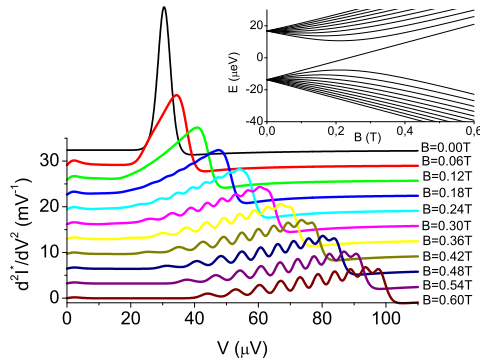


FIG. 3: (Color online) Energy spectrum of ^{232}Bi in Silicon as a function of applied field and the corresponding $\frac{d^2I}{dV^2}$ spectra at $k_B T = 10\text{mK}$.

ergy $E(F) = \frac{A}{2}(F(F+1) - S(S+1) - I(I+1))$. The zero field splitting is as large as $5A \simeq 30\mu\text{eV}$, which could be resolved in IETS at $k_B T \simeq 60\text{mK}$. The evolution of the spectrum as a function of B is shown in Fig. 3. A single Bi dopant in Si could be probed by single spin IETS-STM, recently demonstrated in semiconductor substrates[10] or in a single dopant Silicon nanotransistor [12, 13], both in the sequential regime, for which the dI/dV curve yield the single electron spectral function, with peaks at every one of the 20 energy levels [31], or in the cotunneling regime, described with the effective coupling (1) which yields information of the electronic spin spectral function. In figure 3 we show the evolution of the d^2I/dV^2 curves, as measured either with STM or in a nanotransistor in the cotunneling regime, for different values of B at $k_B T = 10\text{mK}$. It is apparent that transport permits to probe the spin-flip transitions between the Zeeman-split states of the joint electron-nuclear spin system.

In summary, we propose an experimental approach to probe a single nuclear spin using IETS of the hyperfine structure of the electronic spin excitations, extending thereby the range of applicability of IETS. Our simulations show that this technique yields information both about energy levels and the occupation of the nuclear spin states of a ^{55}Mn adatom probed with a STM at 4mK . In the case of a single ^{232}Bi dopant in a Si nanotransistor, the hyperfine structure could be detected at 60mK , well within range of current state of the art.

We acknowledge fruitful discussions with C. Untiedt, C. F. Hirjibehedin and A. F. Otte. This work was supported by MEC-Spain (MAT07-67845, FIS2010-21883-C02-01, Grants JCI-2008-01885 and CONSOLIDER CSD2007-00010) and Generalitat Valenciana (ACOMP/2010/070).

- [1] B. Kane, *Nature* **393**, 133 (1998).
- [2] N. A. Gershenfeld and I. L. Chuang, *Science* **275**, 350 (1997).
- [3] P. Neumann, J. Beck, M. Steiner, F. Rempp, H. Fedder, P. R. Hemmer, J. Wrachtrup, and F. Jelezko, *Science* **329**, 542 (2010).
- [4] A. J. Heinrich, J. A. Gupta, C. P. Lutz, and D. M. Eigler, *Science* **306**, 466 (2004).
- [5] C. F. Hirjibehedin, C. P. Lutz, and A. J. Heinrich, *Science* **312**, 1021 (2006).
- [6] C. Hirjibehedin, C.-Y. Lin, A. Otte, M. Ternes, C. P. Lutz, B. A. Jones, and A. J. Heinrich, *Science* **317**, 1199 (2007).
- [7] A. F. Otte, M. Ternes, K. von Bergmann, S. Loth, H. Brune, C. P. Lutz, C. F. Hirjibehedin, , and A. J. Heinrich, *Nature Physics* **4**, 847 (2008).
- [8] A. F. Otte, M. Ternes, S. Loth, C. P. Lutz, C. F. Hirjibehedin, and A. J. Heinrich, *Phys. Rev. Lett.* **103**, 107203 (2009).
- [9] S. Loth, K. von Bergmann, M. Ternes, A. F. Otte, C. P. Lutz, and A. J. Heinrich, *Nature Physics* **6**, 340 (2010).
- [10] A. A. Khajetoorians, B. Chilian, J. Wiebe, S. Schuwalow, F. Lechermann, and R. Wiesendanger, *Nature* **467**, 1084 (2010).
- [11] J. Fernández-Rossier, *Phys. Rev. Lett.* **102**, 256802 (2009).
- [12] G. P. Lansbergen, G. C. Tettamanzi, J. Verduijn, N. Col-laert, S. Biesemans, M. Blaauboer, and S. Rogge, *Nano Letters* **10**, 455 (2010).
- [13] K. Y. Tan, K. W. Chan, M. Mottonen, A. Morello, C. Yang, J. v. Donkelaar, A. Alves, J.-M. Pirkkalainen, D. N. Jamieson, R. G. Clark, et al., *Nano Letters* **10**, 11 (2010).
- [14] S. De Franceschi, S. Sasaki, J. M. Elzerman, W. G. van der Wiel, S. Tarucha, and L. P. Kouwenhoven, *Phys. Rev. Lett.* **86**, 878 (2001).
- [15] G. P. Berman, G. W. Brown, M. E. Hawley, and V. I. Tsifrinovich, *Phys. Rev. Lett.* **87**, 097902 (2001).
- [16] A. V. Balatsky, J. Fransson, D. Mozyrsky, and Y. Manassen, *Phys. Rev. B* **73**, 184429 (2006).
- [17] Y. Manassen, R. J. Hamers, J. E. Demuth, and A. J. Castellano Jr., *Phys. Rev. Lett.* **62**, 2531 (1989).
- [18] Y. J. Song, A. F. Otte, Y. Kuk, Y. Hu, D. B. Torrance, P. N. First, W. A. de Heer, H. Min, S. Adam, M. D. Stiles, et al., *Nature* **467**, 185 (2010).
- [19] J. A. Appelbaum, *Phys. Rev.* **154**, 633 (1967).
- [20] J. Fransson, *Nano Lett.* **9**, 2414 (2009).
- [21] F. Delgado, J. J. Palacios, and J. Fernández-Rossier, *Phys. Rev. Lett.* **104**, 026601 (2010).
- [22] F. Delgado and J. Fernández-Rossier, *Phys. Rev. B* **82**, 134414 (2010).
- [23] J. Lambe and R. C. Jaklevic, *Phys. Rev.* **165**, 821 (1968).
- [24] J.-P. Gauyacq, F. D. Novaes, and N. Lorente, *Phys. Rev. B* **81**, 165423 (2010).
- [25] M. Persson, *Phys. Rev. Lett.* **103**, 050801 (2009).
- [26] W. M. Walsh, J. Jeener, and N. Bloembergen, *Phys. Rev.* **139**, A1338 (1965).
- [27] O. Guillot-Noël, P. Goldner, Y. L. Du, E. Baldit, P. Monnier, and K. Bencheikh, *Phys. Rev. B* **74**, 214409 (2006).
- [28] H. Ma, , and F. Yang, *At. Data and Nuc. Data Tables* **86**, 18 (2004).

- [29] G. W. Morley, M. Warner, A. M. Stoneham, P. T. Greenland, J. van Tol, C. W. M. Kay, and G. Aeppli, *Nature Materials* **9**, 725 (2010).
- [30] R. E. George, W. Witzel, H. Riemann, N. V. Abrosimov, N. Nötzel, M. L. W. Thewalt, and J. J. L. Morton, *Phys. Rev. Lett.* **105**, 067601 (2010).
- [31] J. Fernández-Rossier and R. Aguado, *Phys. Rev. Lett.* **98**, 106805 (2007).